On a nonlinear approach to uncertainty quantification on the ensemble of numerical solutions

Alekseev A.K.[0000-0001-8317-8688], Bondarev A.E.[0000-0003-3681-5212] and Kuvshinnikov A.E.[0000-0003-1667-6307]

Keldysh Institute of Applied Mathematics RAS, Moscow, Russia
aleksey.k.alekseev@gmail.com, bond@keldysh.ru, kuvsh90@yandex.ru

Abstract. The estimation of the approximation errors using the ensemble of numerical solutions is considered in the Inverse Problem statement. The Inverse Problem is set in the nonlinear variational formulation that provides additional opportunities. The ensemble of numerical results is analyzed, which is obtained by the OpenFOAM solvers for the inviscid compressible flow containing an oblique shock wave. The numerical tests demonstrated feasibility to compute the approximation errors without any regularization. The refined solution, corresponding the mean of numerical solutions with the approximation error correction, is also computed and compared with the analytic one.

Keywords: uncertainty quantification, ensemble of numerical solutions, Euler equations, oblique shock, OpenFOAM, Inverse Problem.

1 Introduction

The standards, regulating the applications of Computational Fluid Dynamics [1,2], recommend the verification of solutions and codes that implies the estimation of the approximation error. By this reason the computationally inexpensive methods for *a posteriori* estimation of the pointwise approximation error are of current interest. We consider herein the computationally inexpensive approach to *a posteriori* error estimation based on the ensemble of numerical solutions obtained by different algorithms [3-5]. This approach may be implemented in a non-intrusive manner using certain postprocessor. The refined solution and the approximation errors are estimated using the combination of solutions at every grid node, which is processed by the Inverse Ill-posed Problem in the variational formulation. The results of the numerical tests for compressible Euler equations are provided. The ensemble of solutions is computed by four OpenFOAM solvers for the inviscid compressible flow. We compare the refined solution and approximation errors computed by Inverse problem with the analytic solution and corresponding error estimates.

ICCS Camera Ready Version 2022
To cite this paper please use the final published version:
DOI: 10.1007/978-3-031-08760-8_52

2 The linear statement for approximation error estimation using the distances between numerical solutions

We consider an ensemble of numerical solutions (grid functions) $u_m^{(i)}$ ($i = 1\ldots n$), computed on the same grid by n different solvers similarly to [3-6]. Papers [3-5] address the estimation of the approximation errors from the differences between solutions and Inverse Problem posed in the variational statement form with the zero order Tikhonov regularization.

A local pointwise analysis of the flowfield is used. The projection of the exact solution $\tilde{u}$ onto the grid is noted as $\tilde{u}_m$, the approximation error for i-th solution is noted as $\Delta u_m^{(i)}$. Here m is the grid point number ($m = 1,\ldots,L$).

Then $N = n \cdot (n-1)/2$ equations that relate the approximation errors and the computable differences of the numerical solutions $d_{ij,m} = u_m^{(i)} - u_m^{(j)} = \tilde{u}_{h,m} + \Delta u_m^{(i)} - \tilde{u}_{h,m} - \Delta u_m^{(j)} = \Delta u_m^{(i)} - \Delta u_m^{(j)}$. The following relations hold for a vectorized form of the differences $f_{k,m}$:

$$D_{kj} \Delta u_m^{(j)} = f_{k,m}\,. \tag{1}$$

Herein, D_{kj} is a rectangular $N \times n$ matrix, the summation over a repeating index is implied (no summation over repeating index m).

The equation (1) has the form:

$$\begin{pmatrix} 1 & -1 & 0 \\ 1 & 0 & -1 \\ 0 & 1 & -1 \end{pmatrix} \begin{pmatrix} \Delta u_m^{(1)} \\ \Delta u_m^{(2)} \\ \Delta u_m^{(3)} \end{pmatrix} = \begin{pmatrix} f_{1,m} \\ f_{2,m} \\ f_{3,m} \end{pmatrix} = \begin{pmatrix} d_{12,m} \\ d_{13,m} \\ d_{23,m} \end{pmatrix} = \begin{pmatrix} u_m^{(1)} - u_m^{(2)} \\ u_m^{(1)} - u_m^{(3)} \\ u_m^{(2)} - u_m^{(3)} \end{pmatrix}. \tag{2}$$

in the simplest case of three numerical solutions.

The solution of system (1) is invariant to a shift transformation $\Delta u_m^{(j)} = \Delta \tilde{u}_m^{(j)} + b$ (for any $b \in (-\infty, \infty)$). By this reason, this problem of approximation error estimation is underdetermined and ill-posed (unstable). A regularization ([7, 8]) is usually necessary in order to obtain the steady and bounded solution of the ill-posed problems. The zero order Tikhonov regularization is used in works [3-5]. It enables to obtain solutions with the minimum shift error $|b|$, since the condition of $\|\Delta u_m\|_{L_2}$ minimum restricts the absolute value of b:

$$\min_{b_m}(\delta(b_m)) = \min_{b_m} \sum_j^n (\Delta u_m^{(j)})^2 / 2 = \min_{b_m} \sum_j^n (\Delta \tilde{u}_m^{(j)} + b_m)^2 / 2\,. \tag{3}$$

One may see that:

ICCS Camera Ready Version 2022
To cite this paper please use the final published version:
DOI: 10.1007/978-3-031-08760-8_52

$$\Delta\delta(b_m) = \sum_j^n (\Delta\tilde{u}_m^{(j)} + b_m)\,\Delta b_m\,, \tag{4}$$

and the minimum of the norm occurs at b_m that equals the mean error (with the opposite sign):

$$b_m = -\frac{1}{n}\sum_j^n \Delta\tilde{u}_m^{(j)} = -\Delta\bar{u}_m\,. \tag{5}$$

Thus, the error $|\Delta u_m^{(j)}|$ cannot be less than $|b_m|$ (the mean error value) in the linear approach. By this reason, the error estimates contain unremovable errors.

The variational statement of the Inverse Problem implies the minimization of the functional:

$$\varepsilon_m(\Delta\vec{u}) = 1/2(D_{ij}\Delta u_m^{(j)} - f_{i,m})\cdot(D_{ik}\Delta u_m^{(k)} - f_{i,m}) + \alpha/2(\Delta u_m^{(j)}\Delta u_m^{(k)})\,. \tag{6}$$

The functional (6) consists of the discrepancy of the predictions and observations and the zero order Tikhonov regularization term (α is the regularization parameter). The efficiency of the linear statement was confirmed by the set of numerical tests presented in papers [3-5].

3 The nonlinear statement for the estimation of the refined solution and the approximation error on the ensemble of numerical solutions

The shift invariance discussed above causes an instability and the presence of unremovable error. Fortunately, this invariance is purely linear effect. So, some transition to the nonlinear statement allows eliminating the shift invariance. Let's consider the corresponding opportunities.

We consider three formulations with the different number of nonlinear terms. The simplest one is presented by equation (7) (and marked as Variant 1):

$$\begin{pmatrix} 2\tilde{u}_m + \Delta u_m^{(1)} & 0 & 0 & \tilde{u}_m \\ 1 & 0 & -1 & 0 \\ 0 & 1 & -1 & 0 \\ 1/3 & 1/3 & 1/3 & 1 \end{pmatrix} \cdot \begin{pmatrix} \Delta u_m^{(1)} \\ \Delta u_m^{(2)} \\ \Delta u_m^{(3)} \\ \tilde{u}_m \end{pmatrix} = \begin{pmatrix} (u_m^{(1)})^2 \\ u_m^{(1)} - u_m^{(3)} \\ u_m^{(2)} - u_m^{(3)} \\ (u_m^{(1)} + u_m^{(2)} + u_m^{(3)})/3 \end{pmatrix}. \tag{7}$$

It contains nonlinear term $\left(u_m^{(1)}\right)^2$ at right hand side that prohibits the shift invariance $u_m^{(j)} = \tilde{u}_m^{(j)} + b$. Additionally, this statement enables a direct estimation of refined solution $\tilde{u}_m$, which corresponds to the average of numerical solutions with account of approximation errors.

ICCS Camera Ready Version 2022
To cite this paper please use the final published version:
DOI: 10.1007/978-3-031-08760-8_52

The solution of Eq. (7) corresponds to the minimum of the following functional (without any regularization and with the dependence of the matrix D_{ij}^m on local parameters):

$$\varepsilon_m(\Delta\vec{u}) = 1/2(D_{ij}^m \Delta u_m^{(j)} - f_{i,m}) \cdot (D_{ik}^m \Delta u_m^{(k)} - f_{i,m}). \tag{8}$$

The nonlinear system (7) is degenerated that can be directly checked. Fortunately, the determinant of matrix operator D_{ij}^m is far from zero. By this reason the linearization of the following form $(D_{ij}^m)^n (\Delta u_m^{(j)})^{n+1} = f_{i,m}$ (n — number of iteration) can be used at the iterative minimization of the functional (8).

The second formulation (variant 2 presented by Eq. 9) contains two nonlinear terms:

$$\begin{pmatrix} 2\tilde{u}_m + \Delta u_m^{(1)} & 0 & 0 & \tilde{u}_m \\ 0 & 2\tilde{u}_m + \Delta u_m^{(2)} & 0 & \tilde{u}_m \\ 0 & 1 & -1 & 0 \\ 1/3 & 1/3 & 1/3 & 1 \end{pmatrix} \cdot \begin{pmatrix} \Delta u_m^{(1)} \\ \Delta u_m^{(2)} \\ \Delta u_m^{(3)} \\ \tilde{u}_m \end{pmatrix} = \begin{pmatrix} (u_m^{(1)})^2 \\ (u_m^{(2)})^2 \\ u_m^{(2)} - u_m^{(3)} \\ (u_m^{(1)} + u_m^{(2)} + u_m^{(3)})/3 \end{pmatrix}. \tag{9}$$

The third formulation (variant 3 presented by Eq. 10) contains all linear terms and all squares of the numerical solutions:

$$\begin{pmatrix} 2\tilde{u}_m + \Delta u_m^{(1)} & 0 & 0 & \tilde{u}_m \\ 0 & 2\tilde{u}_m + \Delta u_m^{(2)} & 0 & \tilde{u}_m \\ 0 & 0 & 2\tilde{u}_m + \Delta u_m^{(3)} & \tilde{u}_m \\ 1 & -1 & 0 & 0 \\ 1 & 0 & -1 & 0 \\ 0 & 1 & -1 & 0 \\ 1/3 & 1/3 & 1/3 & 1 \end{pmatrix} \cdot \begin{pmatrix} \Delta u_m^{(1)} \\ \Delta u_m^{(2)} \\ \Delta u_m^{(3)} \\ \tilde{u}_m \end{pmatrix} = \begin{pmatrix} (u_m^{(1)})^2 \\ (u_m^{(2)})^2 \\ (u_m^{(3)})^2 \\ u_m^{(1)} - u_m^{(2)} \\ u_m^{(1)} - u_m^{(3)} \\ u_m^{(2)} - u_m^{(3)} \\ (u_m^{(1)} + u_m^{(2)} + u_m^{(3)})/3 \end{pmatrix}. \tag{10}$$

The considered nonlinear statement enables the estimation of approximation errors without any regularization. In addition, the refined solution $\tilde{u}_m$ can be computed.

4 The minimization algorithm

We apply the steepest descent iterations (k is the number of the iteration) for the minimization of the functionals (6) and (8):

$$\Delta u_m^{(j),k+1} = \Delta u_m^{(j),k} - \tau \nabla \varepsilon_m. \tag{11}$$

ICCS Camera Ready Version 2022
To cite this paper please use the final published version:
DOI: 10.1007/978-3-031-08760-8_52

The gradient is obtained by the numerical differentiation. The iterations terminate at a small value of the functional $\varepsilon \le \varepsilon_*$ ($\varepsilon_* = 10^{-8}$ was used in these tests).

The solutions depend on the regularization parameter α in the linear statement. At $\alpha = 0$ the magnitude of $\left|\Delta u^{(j)}(\alpha)\right|$ is not bounded. The limit $\alpha \to \infty$ is not acceptable also, since $\left|\Delta u^{(j)}(\alpha)\right| \to 0$. A range of the regularization parameter α exists where the weak dependence of the solution on α is manifested (numerical tests determine it as $\alpha \in (10^{-6}, 10^{-1})$). The solution $\Delta u^{(j)}(\alpha)$ is close to the exact one in this range and may be considered as the regularized solution [8].

5 The test problem

The solutions and the errors considered in the paper correspond to the oblique shock waves, which are chosen due to the availability of analytic solutions and the relatively high level of the approximation errors. The test problem is governed by the two dimensional compressible Euler equations.

The shocked flowfield is engendered by a plate at the angle of attack α = 20° in the uniform supersonic flow (M=4). The results are compared with the projection of the analytic solution on the computational grid.

The inflow parameters are set on the left boundary ("*inlet*") and on the upper boundary *("top"*). The zero gradient condition for the gas dynamic functions is specified on the right boundary ("*outlet*"). The condition of zero normal gradient is posed for the pressure and the temperature, and the condition "*slip*" is posed for the speed, that ensures the non-penetration on the plate surface.

The following solvers from the OpenFOAM software package [9] are used:

- *rhoCentralFoam* (rCF), which is based on a central-upwind scheme [10,11].
- *sonicFoam* (sF), which is based on the PISO algorithm [12].
- *pisoCentralFoam* (pCF) [13], which combines the Kurganov-Tadmor scheme [10] and the PISO algorithm [12].
- *QGDFoam* (QGDF), which implements the quasi-gas dynamic equations [14].

It is important for the problem considered in this paper that these solvers use the quite different algorithms.

We estimate the refined solution and approximation errors by minimizing the functional (8) using Expressions (7),(9),(10). The analytic solution corresponds to the oblique shock wave (Rankine-Hugoniot relations).

6 Numerical results

The Figs. 1 and 3 present the pieces of vectorized grid function of the density obtained by the Inverse Problem in comparison with the exact error. The Figs. 2 and 4 present the pieces of the vectorized density error in comparison with the exact error. The index along the abscissa axis $i = N_x(k_x - 1) + m_y$ is defined by indexes along

ICCS Camera Ready Version 2022
To cite this paper please use the final published version:
DOI: 10.1007/978-3-031-08760-8_52

$X(k_x)$ and $Y(m_y)$. The periodical jump of variables corresponds to the transition through the shock wave. Results for $\alpha = 20°$, $M = 4$ are provided.

The Fig. 1 demonstrates close results for nonlinear estimations of the refined density (Var1, Var2 and Var3) for numerical solutions computed using rCF, pCF and sF algorithms. Var1, Var2 and Var3 correspond to nonlinear estimation of $\tilde{u}_m$ by Eqs (7), (9) and (10). Figure 2 shows that the numerical density errors for linear and nonlinear estimates are close. The error estimates are shifted with respect to the exact error.

The Figs. 3 and 4 provide the density and its errors for the set of numerical solutions, which are computed by rCF, pCF and QGDF solvers. Var1 corresponds to nonlinear estimation of $\tilde{u}_m$ by Eqs (7). The replacement of sF by QGDF weakly affects on the behaviour of variables.

Both linear and nonlinear approaches provide close results for the error estimates. However, nonlinear options (in contrast to linear one) provide the refined solution $\tilde{u}_m$ and do not use any regularization that presents the main advantage of this approach.

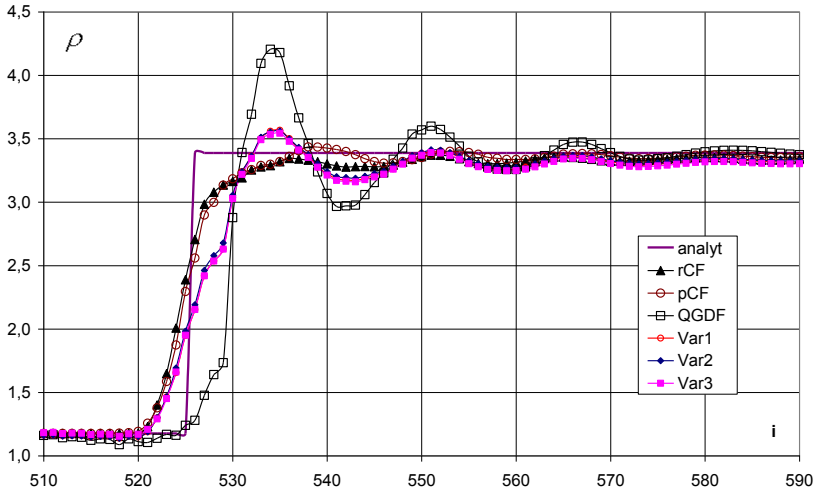

Fig. 1. The vectorized values of the density computed by rCF, pCF, sF, refined solutions obtained by the Inverse Problem (Var1, Var2 and Var3) and the analytic solution.

ICCS Camera Ready Version 2022
To cite this paper please use the final published version:
DOI: 10.1007/978-3-031-08760-8_52

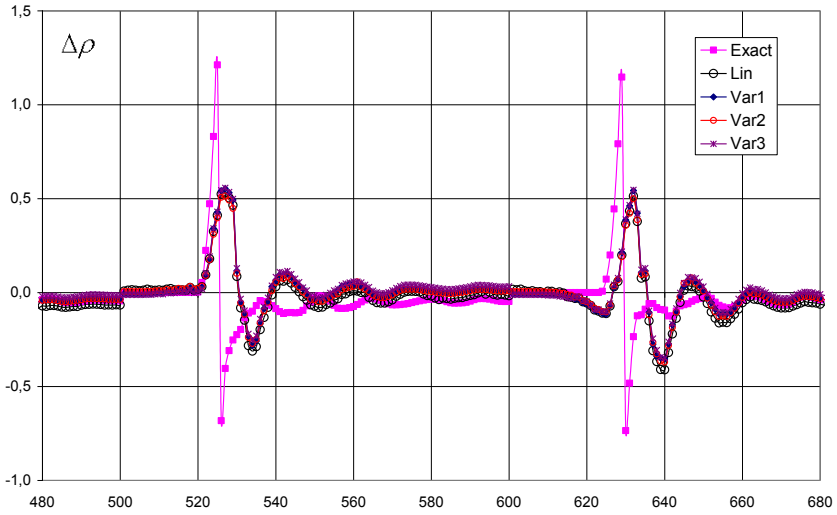

Fig. 2. The vectorized exact density error for solution computed by rCF algorithm, the linear error estimates, and the nonlinear estimates of error (Var1, Var2 and Var3).

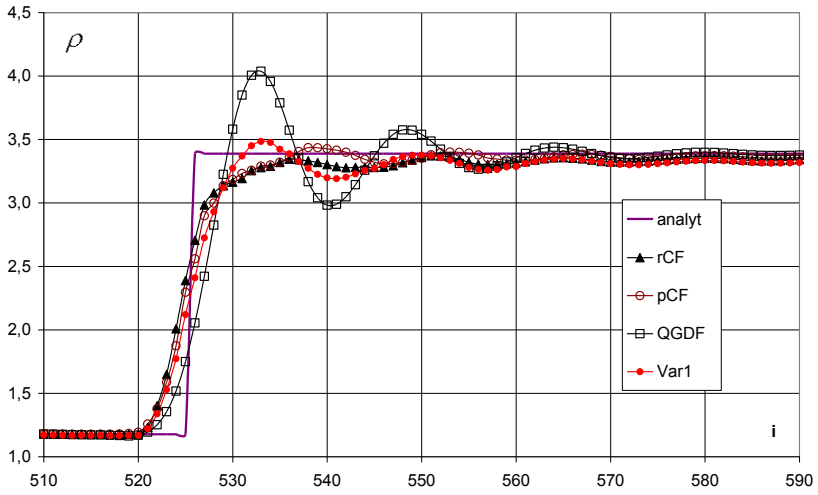

Fig. 3. The vectorized values of the density (rCF, pCF, QGDF), refined solutions, obtained by the Inverse Problem (Var1), and the analytic solution.

ICCS Camera Ready Version 2022
To cite this paper please use the final published version:
DOI: 10.1007/978-3-031-08760-8_52

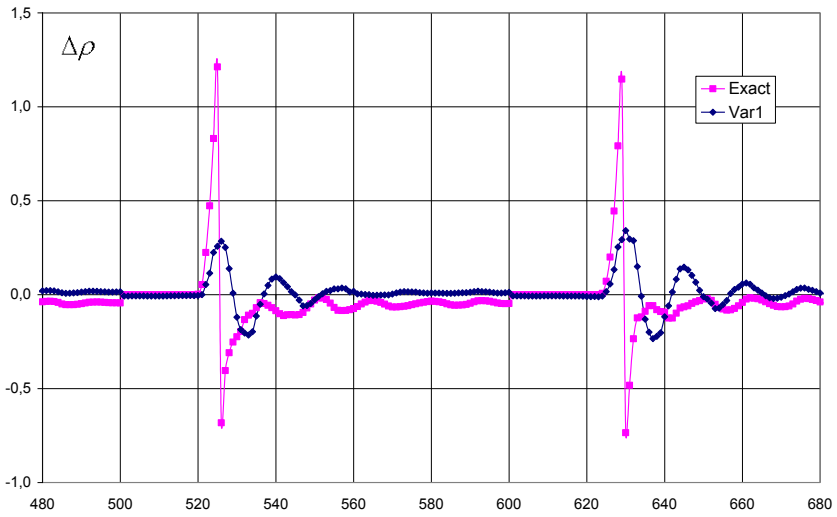

Fig. 4. The vectorized exact density error for solution computed by rCF solver and the nonlinear estimates of error (Var1).

7 Discussion

The Inverse Problem (IP) based approach was used in the linear statement by [3] for the supersonic axisymmetric flows around cones, for the crossing shocks (Edney-I and Edney-VI patterns by [4] and for the oblique shock flow pattern by [5].

Here, we consider a nonlinear extension of IP-based method [3-5] for the oblique shock flow pattern. The analytic solutions and exact errors (obtained by the comparison with the analytic solutions) are used as the etalons.

No regularization is used at the nonlinear case in contrast to the linear statement [3-5]. This circumstance is caused by the nonlinearity that prevents from the linear shift invariance that is specific for the linear statement.

Additionally, the nonlinear option enables the explicit estimation of the refined solution $\tilde{u}_m$. At first glance, it seems to be impossible to obtain four independent variables $\tilde{u}_m$, $\Delta u_m^{(1)}$, $\Delta u_m^{(2)}$, $\Delta u_m^{(3)}$ using three input parameters $u_m^{(1)}$, $u_m^{(2)}$, $u_m^{(3)}$. The unexpected success of the nonlinear approach may be caused by implicit correlations between $\tilde{u}_m$ and $\Delta u_m^{(i)}$ that are contained in the input data $u_m^{(i)}$. The correlations between $\Delta u_m^{(i)}$ really exist and are demonstrated by [6]. One of the reasons for these correlations is the similar behaviour of the approximation errors at discontinuities, see Fig. 5.

ICCS Camera Ready Version 2022
To cite this paper please use the final published version:
DOI: 10.1007/978-3-031-08760-8_52

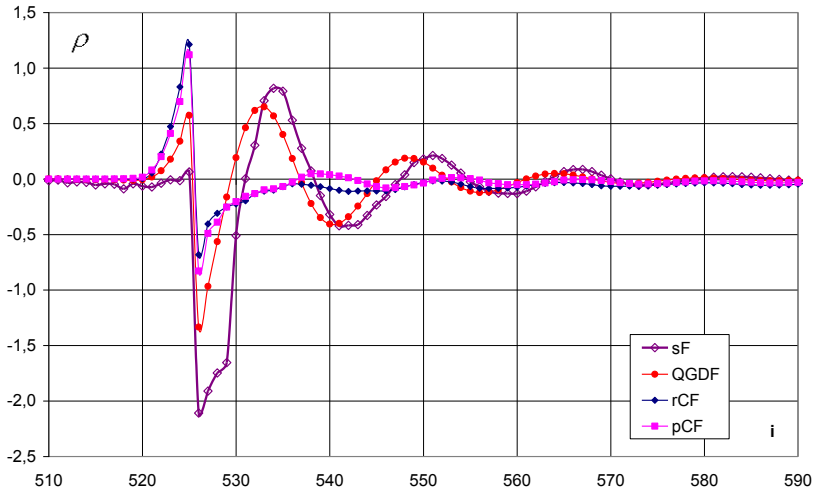

Fig. 5. The correlated nature of approximation errors in the vicinity of shock wave.

However, the additional analysis of the advantages and limitations of the nonlinear version is necessary.

8 Conclusion

An ensemble of numerical solutions obtained by different methods is considered for estimation of the pointwise refined solution and the approximation errors. The post-processing is applied, which is based on the Inverse Problem. The linear and nonlinear statements are analyzed and compared.

The nonlinear approach (in contrast to linear one) provides the estimation of the refined solution $\tilde{u}_m$, does not use any regularization, and, formally, has no limitations on the accuracy of error estimation that is specific for linear approach [3-5].

The four solvers from the OpenFOAM software package are used in numerical experiments. The two-dimensional inviscid flow pattern engendered by the oblique shock wave is considered as a test case.

The numerical tests demonstrate the successful estimation of the refined solution and the pointwise approximation error in the nonlinear statements.

References

1. Guide for the Verification and Validation of Computational Fluid Dynamics Simulations, American Institute of Aeronautics and Astronautics, AIAA-G-077-1998, 1998.
2. Standard for Verification and Validation in Computational Fluid Dynamics and Heat Transfer, ASME V&V 20-2009, 2009.

ICCS Camera Ready Version 2022
To cite this paper please use the final published version:
DOI: 10.1007/978-3-031-08760-8_52

3. Alekseev, A.K., Bondarev, A.E., Kuvshinnikov, A.E.: A posteriori error estimation via differences of numerical solutions, in V. V. Krzhizhanovskaya et al. (Eds.): ICCS 2020. Lecture Notes in Computer Science (LNCS), vol. 12143, pp. 508–519. Springer, Cham (2020). https://doi.org/10.1007/978-3-030-50436-6_37
4. Alekseev, A.K., Bondarev, A.E.: The Estimation of Approximation Error using Inverse Problem and a Set of Numerical Solutions, Inverse Problems in Science and Engineering. 29 (13), 3360–3376 (2021). https://doi.org/10.1080/17415977.2021.2000604
5. Bondarev, A.K., Kuvshinnikov, A.E.: A Comparison of the Richardson Extrapolation and the Approximation Error Estimation on the Ensemble of Numerical Solutions. In: Paszynski M., Kranzlmüller D., Krzhizhanovskaya V.V., Dongarra J.J., Sloot P.M.A. (eds) Computational Science – ICCS 2021, Lecture Notes in Computer Science, vol. 12747. pp. 554-566. Springer (2021). https://doi.org/10.1007/978-3-030-77980-1_42
6. Alekseev, A.K., Bondarev, A.E.: On a posteriori error estimation using distances between numerical solutions and angles between truncation errors. Mathematics and Computers in Simulation 190, 892–904 (2021). https://doi.org/10.1016/j.matcom.2021.06.014
7. Tikhonov, A.N., Arsenin, V.Y.: Solutions of Ill-Posed Problems. Winston and Sons, Washington DC (1977).
8. Alifanov, O.M., Artyukhin, E.A., Rumyantsev S.V.: Extreme Methods for Solving Ill-Posed Problems with Applications to Inverse Heat Transfer Problems. Begell House (1995).
9. OpenFOAM, http://www.openfoam.org. Accessed 20 Jan 2022
10. Kurganov, A., Tadmor, E.: New high-resolution central schemes for nonlinear conservation laws and convection-diffusion equations. J. Comput. Phys. 160(1), 241–282 (2000). https://doi.org/10.1006/jcph.2000.6459
11. Greenshields, C., Wellerr, H., Gasparini, L., Reese, J.: Implementation of semi-discrete, non-staggered central schemes in a colocated, polyhedral, finite volume framework, for high-speed viscous flows. Int. J. Numer. Meth. Fluids 63(1), 1–21 (2010). https://doi.org/10.1002/fld.2069
12. Issa, R.: Solution of the implicit discretized fluid flow equations by operator splitting. J. Comput. Phys. 62(1), 40–65 (1986). https://doi.org/10.1016/0021-9991(86)90099-9
13. Kraposhin, M., Bovtrikova, A., Strijhak, S.: Adaptation of Kurganov-Tadmor numerical scheme for applying in combination with the PISO method in numerical simulation of flows in a wide range of Mach numbers. Procedia Computer Science 66, 43–52 (2015). https://doi.org/10.1016/j.procs.2015.11.007
14. Kraposhin, M.V., Smirnova, E.V., Elizarova, T.G., Istomina, M.A.: Development of a new OpenFOAM solver using regularized gas dynamic equations. Computers & Fluids 166, 163–175 (2018). https://doi.org/10.1016/j.compfluid.2018.02.010

ICCS Camera Ready Version 2022
To cite this paper please use the final published version:
DOI: 10.1007/978-3-031-08760-8_52